

## Utilization of Landsat and Field Data in Geological Mapping of Vom-Kuru Area, North-central Nigeria

E.Y. Yenne<sup>1\*</sup>, D.A Bala<sup>2</sup>, I.E. Abalaka<sup>3</sup>, T.M Ozoji<sup>4</sup>, L.W Nimze<sup>5</sup>

1, 3, 5. Department of Geology, University of Jos, P.M.B 3084, Jos, Nigeria

2. Department of Science Laboratory Technology, University of Jos, Jos, Nigeria.

4. Department of Geology and Mining, Ibrahim Badamasi Babangida University Lapai, Niger State, Nigeria.

### Abstract

The study area is a part of the Jos-Bukuru younger granite ring complex of North-central, Nigeria. It is very difficult to carry out geological mapping due to its rugged terrain as well as difficulty in accessing several outcrops due to communal conflicts. In view of this, the study integrated Landsat and field data to precisely map out the geology of the area. Five (5) land cover elements i.e. soil minerals, drainage pattern, surface water bodies, vegetations and rock outcrops were successfully mapped out from Landsat data. Thus, mafic and granitic rocks were observed and classified as rock units. One hundred and twenty-four (124) lineaments were automatically extracted in PCI Geomatica software and analyses show that they trend majorly in a North-south direction. Seventeen (17) rock samples were obtained in the field; they were studied and analyzed, and was observed that four (4) basic rocks units occurred in the area: basalt, biotite microgranite, biotite granite and undifferentiated older (porphyry) granite. Furthermore, five (5) groundwater samples were analyzed for major cations and anions elements using Atomic Absorption Spectrometer (AAS) and the result indicated the presence  $\text{Ca}^{2+}$ ,  $\text{Mg}^{2+}$ ,  $\text{Na}^+$ ,  $\text{K}^+$ ,  $\text{HCO}_3^-$ ,  $\text{SO}_4^{2-}$  and  $\text{Cl}^-$  where the concentration of  $\text{Na}^+/\text{K}^+$  ions are greater than  $\text{Ca}^{2+}/\text{Mg}^{2+}$  while which  $\text{HCO}_3^-$  is greater than  $\text{Cl}^-/\text{SO}_4^{2-}$  and as such the alkali-bicarbonate dominated the composition of the groundwater. This result proved valid that the geology of the study area is composed predominantly of rocks that are mainly alkaline in nature and this also correlated with the result of the geology obtained from remotely sensed data as well as from fieldwork. Therefore, the study has shown that the area is composed of basically two (2) main rock types: mafic rocks (basalts), felsic rocks (biotite microgranite, biotite granite and undifferentiated older porphyry granite).

**Keywords:** Atomic Absorption Spectrometer, alkaline-bicarbonate, Landsat, Landcover, Lineaments, geology

### 1. Introduction

There has been dear need for the integration of several research methods in geology so as to adequately describe and reconstruct the environment for proper developmental plans. This quest brought to light the introduction of remote sensing in geology in order to supplement other old processes like field mapping. Remote Sensing being the science and art of obtaining information about an object and/or area through the analysis of data acquired by a device that is not in contact with the object and/or area under investigation (Lillesand and Kiefer, 1994), has shown over the years to be vital in geological investigations. Thus, specific remote sensing methods and data have been developed and this has formed a critical part of geological mapping over the years. In view of the importance of remote sensing, many scientists have statistically selected Landsat TM enhanced false colour composite and used it to map geological terranes with high degree of confidence (Drury and Berhe 1993; Souza Filho and Drury 1997; Carranza *et al.*, 2002). Remote sensing techniques usually offer a medium for a successful discrimination and mapping of exposed rocks and associated weathering products, providing information that is relevant to maps of bedrock geology (Rowan *et al.*, 2005; David and Woolf, 2012). Usually, it's the reflectance characteristics of individual lithological classes (*i.e.*, rock or soil types) that are mainly used as function of the presence of minerals to be utilized. It is essential to note that Landsat bands 4, 5, and 7 are most successfully used to discriminate between major rock types (Rothery 1987). This can be achieved through several processes but the most important one here is band ratioing which has been used successfully in lithological mappings. Many scientists have successfully employed band ratios and its composite images in discriminating and identifying different rock types (Adam and Felic, 1967; Sultan *et al.*, 1987; Drury 1993; Sabins, 1996; Souza Filho and Drury, 1997; Sabreen and Timothy, 2006). Band ratios are prepared by dividing digital numbers of each pixel in one band by another pixel of the other band which acts as denominator and this depends on the rock reflectance properties (Qari *et al.*, 2007, Mshiu, 2011). Thus, the application of remote sensing can be limited when it comes to interpretation of geological and structural data where different surface conditions such as vegetation, agricultural activities and weathering may act as hindrance to a successful outcrop capture (Drury, 1993). Therefore, remotely sensed data no matter how sophisticated require ground truthing in the form of field work for verification prior validation. The ground truthing phase allows the expertise and the intellectual endowment of the geologist to be at interface with the geological feature, to guarantee the most reliable results (Malomo, 2009). Therefore, Landsat data analyses for lithological mapping should always be correlated and

evaluated with available fieldwork.

The study area has a very rugged and difficult terrain due to the undulating nature of the area as a result of the intrusion of younger granite as well as the incessant communal conflicts within the study area. Hence, this research is aimed at combining remote sensing and field data in accurate geology mapping of the study area since remote sensing techniques allows a very quick access to an area with precise targets for rock samplings.

## 2. The Study Area

The area under study is Vom-Kuru and its environs. It lies between longitude  $8^{\circ} 45' 0''$ E and  $8^{\circ} 50' 0''$  E; and latitude  $9^{\circ} 40' 30.0''$ N and  $9^{\circ} 50' 30.0''$ N covering  $20 \text{ Km}^2$  (Figure 1). The area is part of the Jos-Bukuru ring complex of the North-central Nigeria composed of three basic rock types: the Basement complex, the Younger Granite and Metavolcanic/volcanic rocks (Mackay *et al.*, 1947). The younger granites being Jurassic to Triassic in age intruded the Precambrian Basement complex of Pan Africa age or older granites with the Tertiary-Quaternary volcanic rocks associated with both rocks. This area is very accessible through Bukuru-Mararaba-Jama'a and Vom-Manchok roads and several other secondary roads like Sabon Gida and Kwal roads. The climatic condition of the area is characterized by two distinct and contrasting climatic conditions; the dry season and the raining season. The average temperature fluctuates between  $20^{\circ}\text{C}$  and  $27^{\circ}\text{C}$ . The vegetation of the study area lies within the Guinea Savannah vegetation zone, characterized by sparsely distributed shrubs and trees. The topography is very rough with irregular relief characterizing the study area due to the intrusion of the basement rocks by the younger granites resulting in an average elevation of 1,200m. The main watershed roughly follows the longer axis of the granite from Kuru in the South through Bukuru to Laminga. This however encourages physical weathering and structural manifestation in the area. The Jos- Plateau, as an isolated upland massif has a naturally developed dendritic pattern of drainage which flows into four major river system: Delimi, Gongola, Benue and Kaduna (Macleod *et al.*, 1971). This area is inhabited by the Beroms, Hausa-Fulani, Igbo etc. The encouraging climatic conditions of the study area provide an enabling environment for the formation of soil type that is very important in growing crops. The soil types of the study area range from reddish brown to-loamy soils. Dark-rich and fertile soils are found on the Vom Area where they are derived from weathered basalts. These soils are very fertile and mainly used is for agriculture.

### 2.1 Geology Settings

The Jos-Bukuru Complex lies at the focal point of younger granite magmatic activities. Many works have shown that there were three major groups of granites; Hornblende-pyroxene-fayalite granite, Biotite granite and Riebeckite granite (Falconer, 1921 and Mackay *et al.*, 1949). Macleod *et al.*, 1971 suggested that the rocks have been directly succeeded by a volcanic cycle and observed many of the initial ring-fractures to have controlled the distribution of the volcanic eruptions. In fact, the Jos-Bukuru complex is elliptical in surface plan with the longer axis extending for a distance of about 30miles from the Shere hills in the northeast to the south around Forum River. The younger granites crosscut the alkali granites and these are characterized by chilling margins against their country rocks (Falconer and Raeburn, 1923; Mackay *et al.*, 1949; Jacobson *et al.*, 1958; Bowden and Turner, 1974; Macleod and Berridge, 1971). The north-south trend of the younger granite intrusive belt has been influenced structurally by the general N-S trend, NNW and NNE alignments parallel to zones of shearing. This result in the Plateau lying discontinuously in the basement, to the west is of the N-S structural trend but to the east are NE-SW and EW structures. This structural trend has made the fracturing and faulting of the country rocks to be a suitable host for groundwater.

## 3. Methodology

The methodology involved the use of remote sensing data aimed at establishing an overview of the area for reconnaissance study followed by geological field work. In the remote sensing method, Landsat 7 ETM<sup>+</sup> and Shuttle Radar Topographic Mission (SRTM) DEM data (all of Path 188 and Row 053 and orthorectified) were acquired from Global Land Cover Facility homepage (<http://glcf.umd.edu/data>) and processed using different processing methods like sub-setting, filtering, density slicing, pan-sharpening, band combination, band ratioing etc. The SRTM DEM data was employed to extract drainage map of the study area through a sequential process of fill, flow direction, flow accumulation, snap pour point, stream order and stream to feature modules in the hydrology ArcToolbox of ArcGIS<sup>®</sup> software. Colour band composite of the subsetted area in the form R: 4, G: 3, B: 1 was displayed and the blue tone pixels which represent surface water bodies were digitized. Also, band ratios in ENVI 4.3<sup>®</sup> were transformed (band ratio 5:7 and band ratio 5:4) in order to pick and analyzed the bands for lithology assessment. However, the spectral signatures of the products of bands ratio 5:7 and 5:4 tend to show similar results as that of vegetation. Therefore, further analysis was carried out so as to show and differentiate the presence of vegetation from other land covers by employing the transformation module of Normalized Difference Vegetation Index (NDVI). The digitized and generated maps were integrated in ArcGIS<sup>®</sup> software where basic land covers were exposed as reconnaissance elements. Henceforth, specific band ratios

and colour band combinations were carried out for possible mafic and felsic rocks delineation in the form of 5/7: 5/1: 3/4 and 5/1: 5/7: 5/4 respectively. The various digitized maps were then integrated to form the generalized land cover map with possible areas of rock unit exposures. An automated lineament extraction method was carried out in PCI geomatica software using Lansat band 8 Panchromatic with 15m resolution. A modeler line user defined parameter was used for optimum lineament extraction over the area. These parameters included edge detection, threshold and linear feature extraction. The extracted lineament was then exported into Rockwork<sup>®</sup> software where the bearings of each lineament was determined and used to plot a rose diagram so as to show the orientations of structures in the area. The lineament map was the draped on the generated remote sensing geology map of the area.

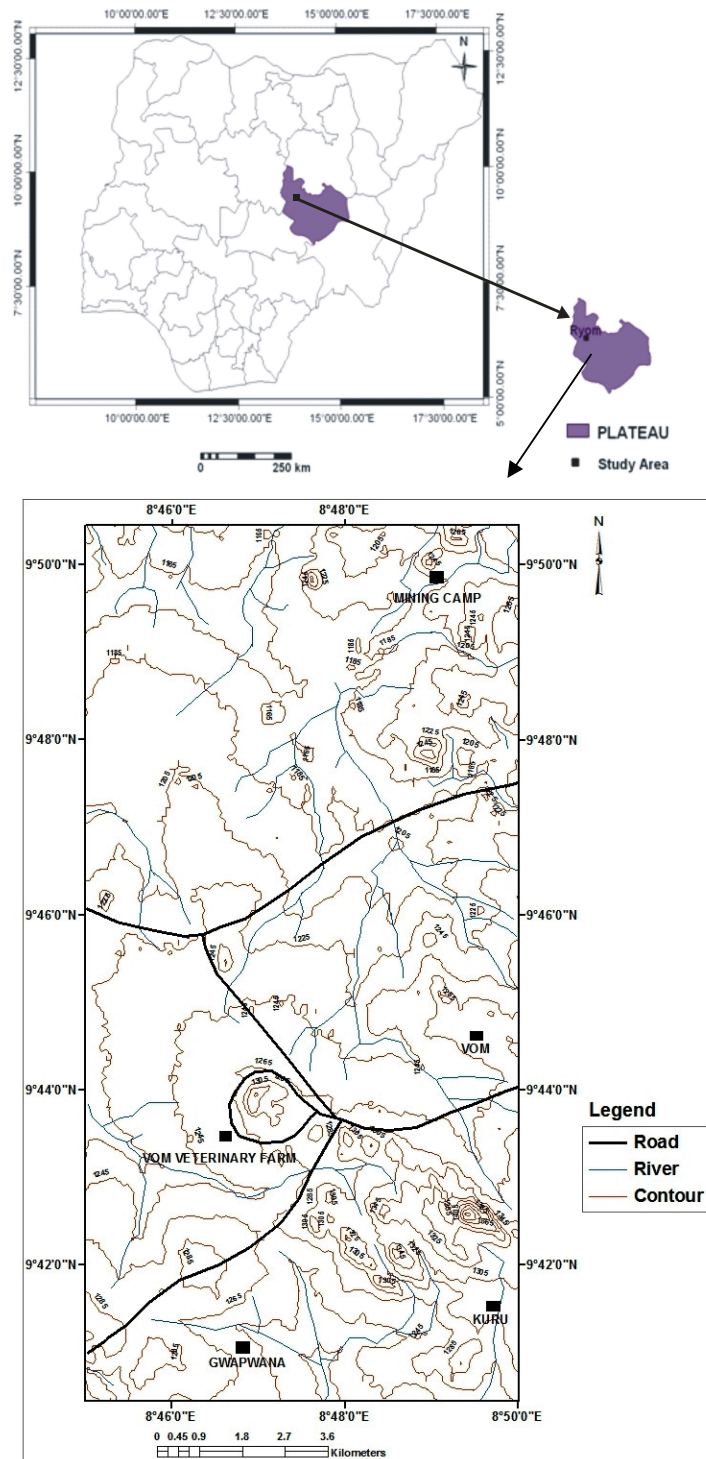


Figure 1: Location of the study area

Subsequently, the produced geology map obtained from remote sensing was ground-truthed by field mapping. In order to achieve a successful field work, planning and preliminary studies of the area as well as a thorough study of the produced geology map from remote sensing was done. Detailed field mapping including traversing, sampling and field petrography descriptions of intrinsic rock structures using brutton compass/clinometers, global positioning system (G.P.S), geological and sledge hammers, tape and ruler, camera, field notebook, hand lens etc was carefully embarked upon. Sampling was done randomly from different locations in the field and thin sections were prepared, examined, analyzed and various minerals were identified, studied and named in the laboratory using petrologic microscope. Again, five (5) groundwater samples were collected with a bucket from wells and stored in 2 litres sampling bottles after treatment. Physical parameters such as temperature, conductivity and the pH were measured with the aid of a pH meter. The water samples were analyzed for major elements using Atomic absorption spectrometer (AAS) in National Metallurgical Development Center (NMDC), Jos, in order to determine the petrogenesis of the rocks. This method works on the principle of comparative method of analysis, in which absorbance is measured as the difference in the transmitted signal of a solution. The instrumentation for AAS equipment consists basically of a line source, hollow cathode lamp, flame atomizer, monochromator, nebulizer and photo detector. The water samples were aspirated (dispersed) into vapour by means of a flame. Sharp spectral lines of various elements in the sample were then generated. Hence, various wavelengths were absorbed so as to allow specific identification of the element of interest whereby the proportion of the light absorbed is measure of the concentration of the element in the vapour. The light source provides exactly the energy for transmitting the analyzed elements from ground state to an excited state. Associated unabsorbed radiation is passed through a monochromator for isolation of spectral lines and then unto the photo-detector (photomultiplier tube). Positive inert gases are produced from an electrical discharge between the electrons connected to a power supply. This positive ion bombarded the cathode sputtering atoms of the metal and the atomic vapour of the metals of interest was produced. Hence, only the wavelength of the elements of interest emitted by the hollow cathode source is absorption and measured on the photo-detector. The amount of absorption is proportional to the concentration of the element in the Vapour. The results were plotted on a piper trilinear diagram and water type was classified appropriately.

#### 4. RESULTS AND DISCUSSIONS

The results obtained were from Landsat data analyses as well as from geological field mapping which is a confirmatory method aimed at producing an accurate geology map of the study area.

##### 4.1 Remote sensing results

Figures 2a and 2b show SRTM DEM data used in production of drainage map of the study area. The drainage map of this area is dendritic in nature implying a crystalline type of environment. Generally, the flow direction of the river channels is towards the northern part of the area. This invariably indicates that the topography is undulating with highest points around Vom and National Veterinary Research Institute (NVRI). A false colour combination of the study area indicates some areas to be greenish implying the presence of vegetation, brownish areas are possibly non-vegetated areas and the bluish areas show typical water bodies (Figures 3a and 3b). Surface water bodies in the study area are small reservoirs of water that shows absence of rock exposures. The river network most at times drains its content into the reservoir which do not allow out-flow and as such a vital area for the study of element in the area since water weather rocks, transport it and deposit it into the surface water bodies. Figures 4a and 4b show a band ratio 5:7 which is usually associated with clays/hydroxyl minerals that have high reflectance in band 5 and high absorption of radiations in band 7 (Darning, 1998 and Qari *et al.*, 2007). Therefore, clay-rich rocks are clearly identified using these bands as they appear as light pixels in gray scale tones. However, iron-rich rocks were identified using ratio of Landsat TM bands 5/4 where rocks associated with iron minerals have high reflectance in band 5 and high absorption of radiations in band 4 (Mshiu, 2011). Hence, those bright tones are indicative of iron rich rocks (Figure 5a and 5b). When the band ratios were combined in 5/4\*5/7 and colour ramped respectively, the area shows two distinct mineral composition i.e. the clay-rich (red speckles) and iron-rich (blue speckles) minerals (Figures 6a and 6b). Thus, the study area shows rocks that are highly rich in Fe and clay minerals. However, in the mineral spectrum, there is an overlap between the oxide and hydroxyl reflectance and reflectance from vegetations; the two groups both have high reflectance in band 4, band 5 and band 7 as in vegetation. This interference is a barrier and normally makes the whole process of Landsat data analysis quite difficult. However, the Normalize Difference Vegetation Index (NDVI) analysis was carried out in which area with bright tones show the presence of vegetation cover and dark tones for those of bare soils and rocks (Figures 7a and 7b). A combination of the generated map from the analyses above gave an overlap of the basic land cover of the area (Figure 8).

Figures 9a and 9b show band ratio images combined in (5/7: 5/1: 3/4) and the extracted areas with the red patches represent abundant hydroxyl minerals. In Sultan *et al.*, (1987) false colour composite (FCC) image (TM3/TM4:Blue, TM5/TM1:Green, TM5/TM7:Red) helps in mapping specific rocks having abundant hydroxyl

minerals with high TM5/TM7 appear as red. Hence, a deeper red tone of the image indicates great content in Fe-bearing aluminosilicates (Souza Filho and Drury, 1997). Usually, Clay minerals that carry hydroxyl groups (OH<sup>-</sup>), derived from their origin through aqueous alteration of aluminosilicate minerals are commonly produced by hydrothermal alteration of mafic minerals (Clark, 2015). Therefore, the red patches are possible areas of mafic rocks. Figures 10a and 10b indicate band ratios images in the colour composite of 5/1: 5/7: 5/4 for the analysis of felsic rocks. Granitic rocks with low opaques (high TM5/TM1), hydroxyl-bearing phases (low TM5/TM7) and Fe-bearing aluminosilicates (low TM5/TM4) show as green hues (Sultan *et al.*, 1987) as well as show intermediate to high ratios on TM5/TM7 and TM5/TM4 as a mixture of hues between cyan and magenta for felsic rocks respectively. Hence, the patches designated as magenta represent portions of possible granitic rocks. Figure 11 gave a summarized land cover of the area with the aim of exploring suitable areas for geological mapping. Parameters generated automatically were employed in the extraction of lineaments of the study area PCI Geomatica (Table 1). Landsat band 8 panchromatic is very efficient in the extraction of lineaments for structural orientation (Figures 12a and 12b). Analyses of the lineament with a rose diagram show that they trend majorly in N-S trend conforming to the general younger granite orientation of the area (Figure 13). Figure 14 show an overview of the geology of the study area where two distinct lithologies have been delineated; the mafic and the felsic rock units. The mafic rock units are basically found at the center towards Vom veterinary farm while the felsic outcrops are found towards the north-east and south-east portions of the area. Integration of all the generated maps gave a fair land cover representation of the study area and as such a viable clue for areas of rock unit exposures and to a larger extent suitable sampling points.

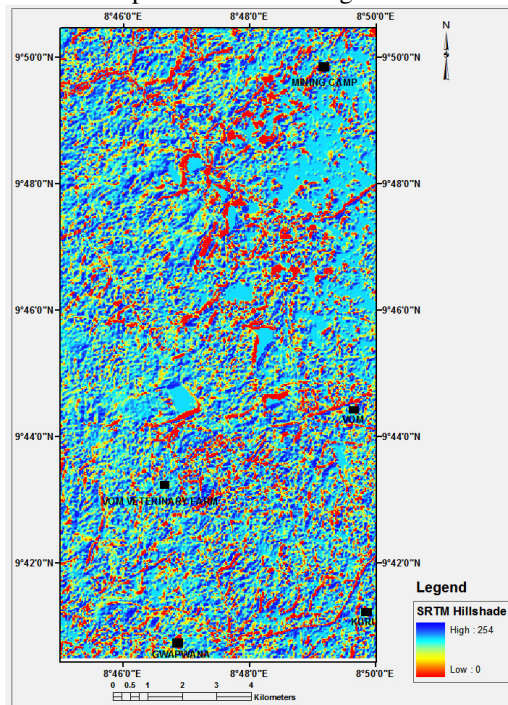


Figure 2a: SRTM Hillshade

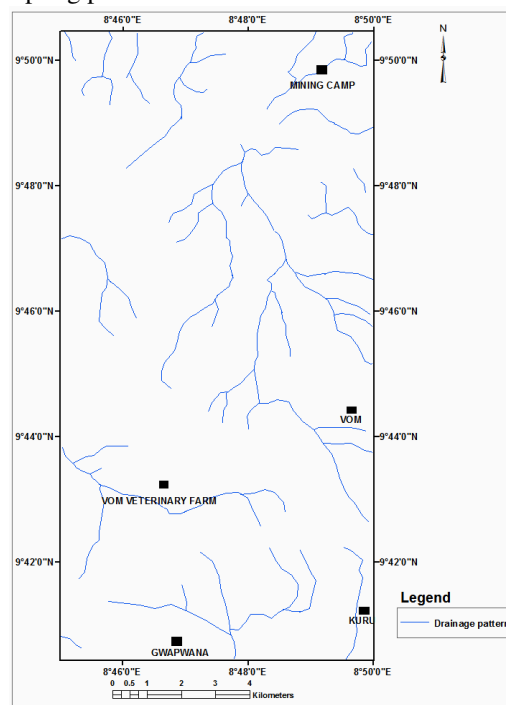


Figure 2b: Drainage map

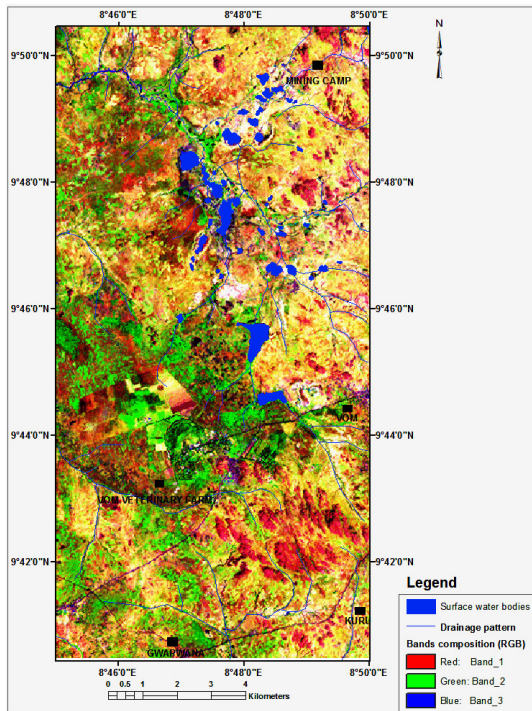


Figure 3a: False band composite

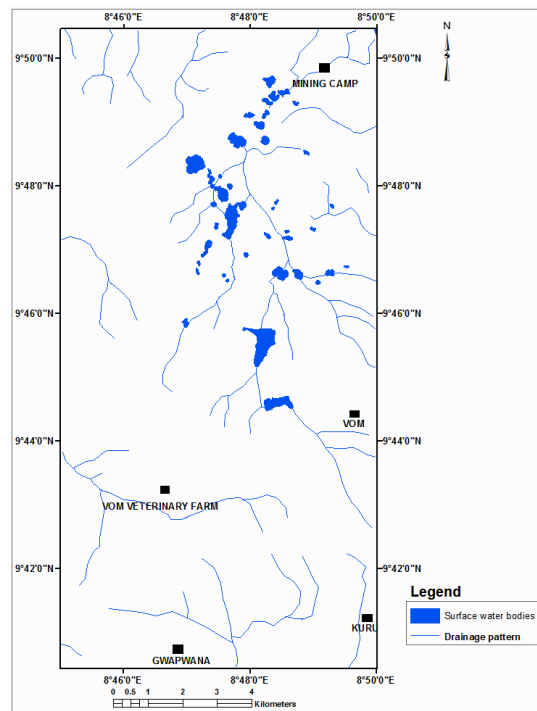


Figure 3b: Extracted surface water bodies

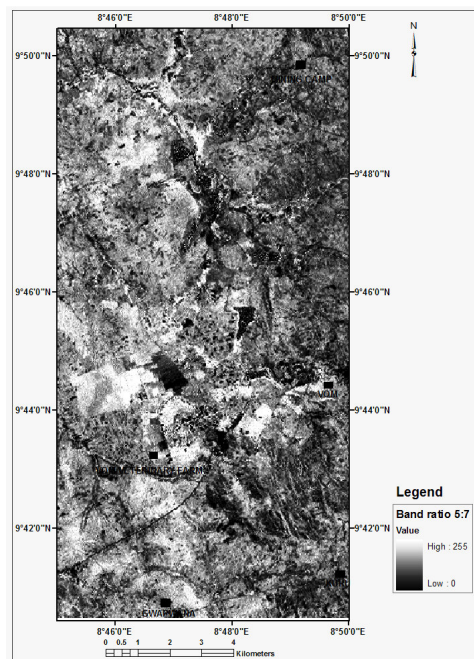


Figure 4a: Band ratio 5/7 (clay-rich minerals)

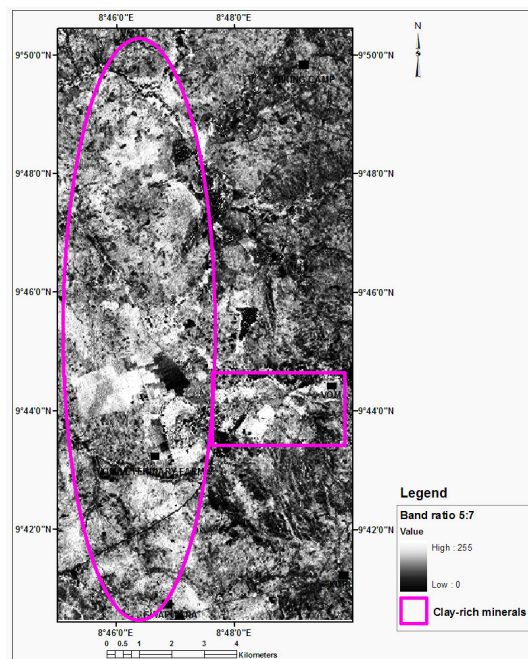


Figure 4b: Areas rich in Clay minerals

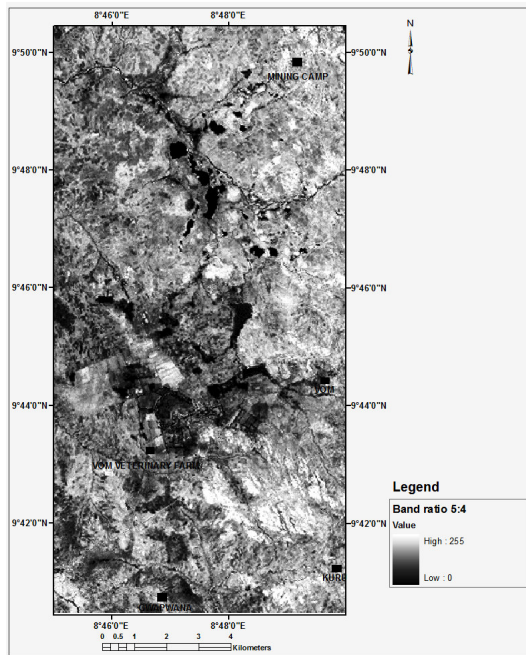


Figure 5a: Band ratio 5/4 (Iron-rich minerals)

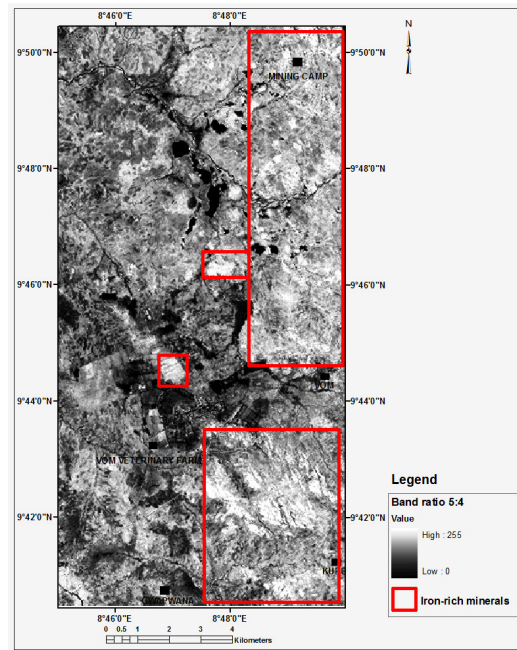


Figure 5b: Areas rich in Iron minerals

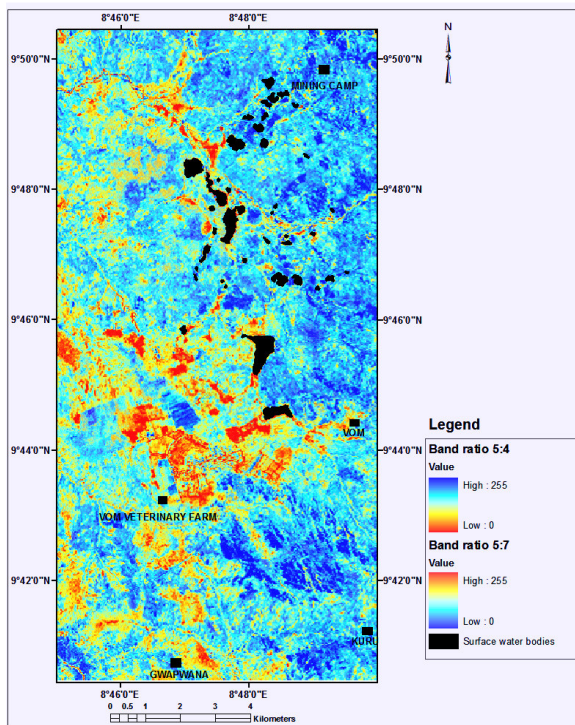


Figure 6a: Combination of 5/4\*5/7

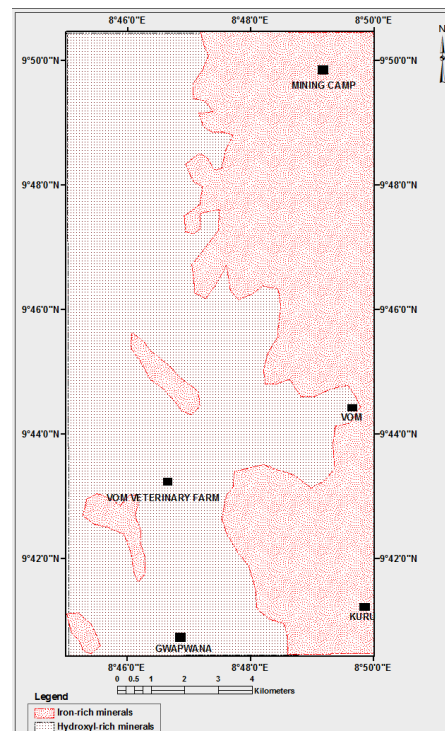


Figure 6b: Digitized generalized lithology

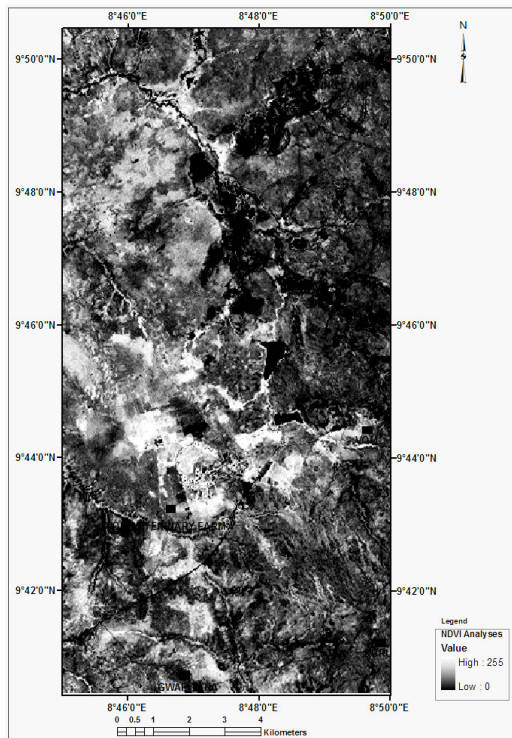


Figure 7a: NDVI (bright pixels show vegetation)

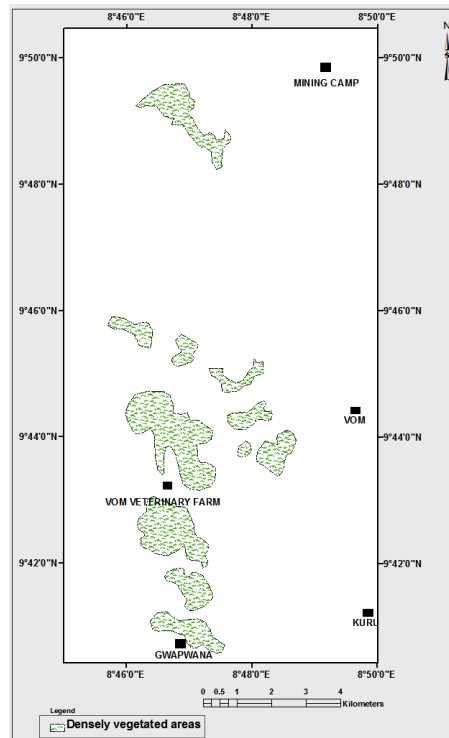


Figure 7b: Digitized NDVI

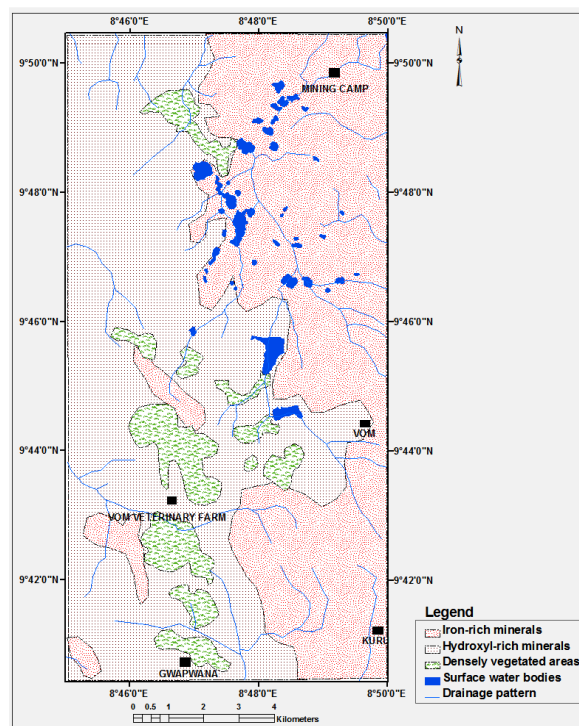


Figure 8: Land cover of the area from remote sensing

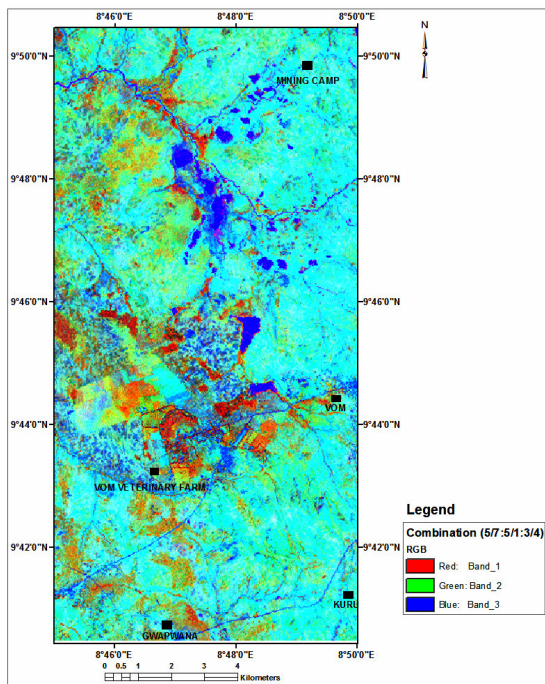


Figure 9a: Colour combination (5/7: 5/1: 3/4)

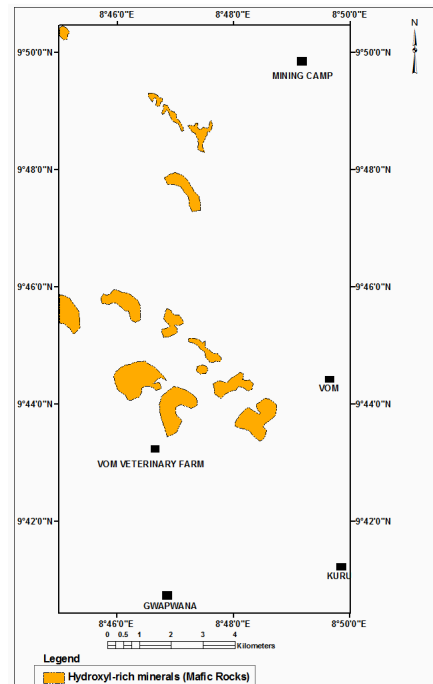


Figure 9b: Digitized mafic rocks area

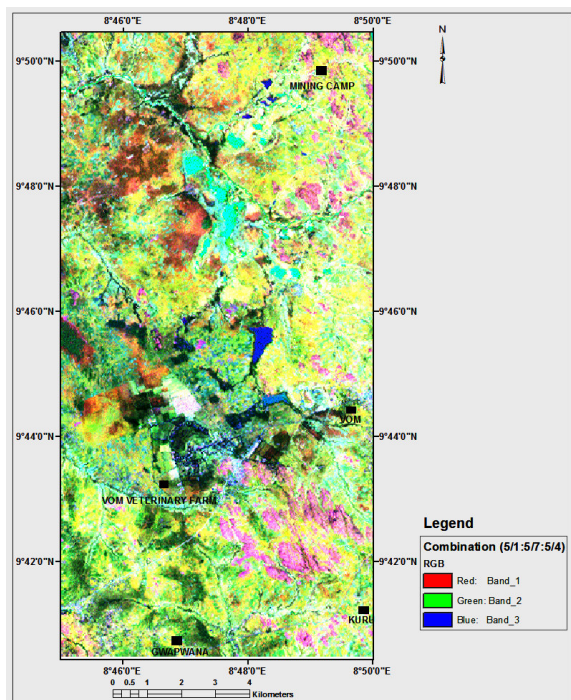


Figure 10a: Colour combination (5/1: 5/7: 5/4)

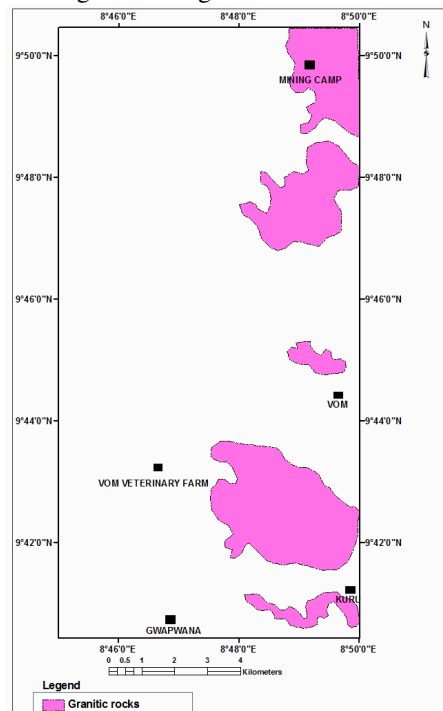


Figure 10b: Digitized Granitic rocks area

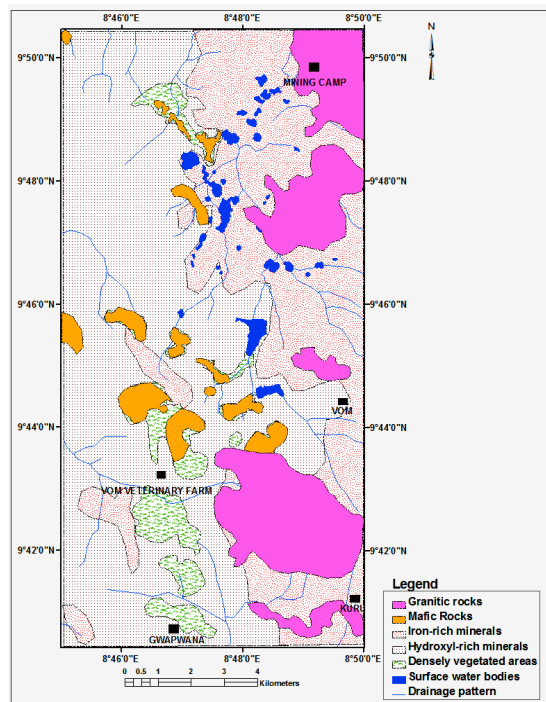


Figure 11: Land cover with possible rock outcrops

Table 1: PCI Geomatica Automatic Lineaments Extraction parameters

PARAMETER	VALUE
Filter Radius (Pixels)	10
Edge Gradient Threshold	100
Curve Length Threshold (Pixels)	30
Line Fitting Error Threshold (Pixels)	3
Angular Difference Threshold (Degrees)	30
Linking Distance Threshold (Pixels)	2

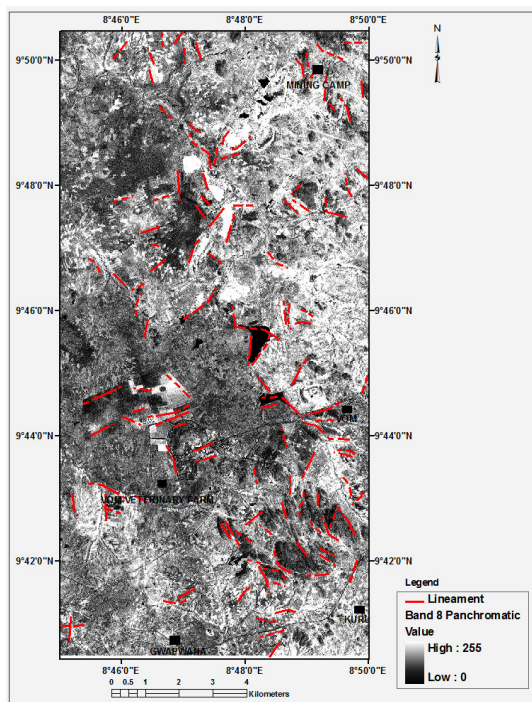


Figure 12a: Lineament draped on band 8

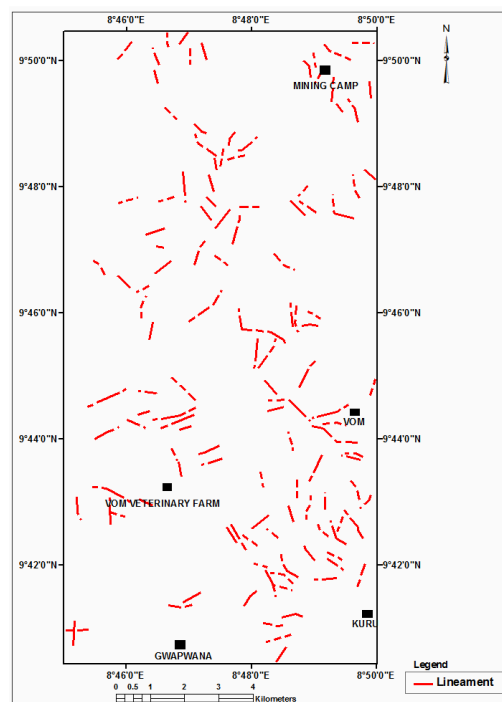


Figure 12b: Automatic lineament extraction

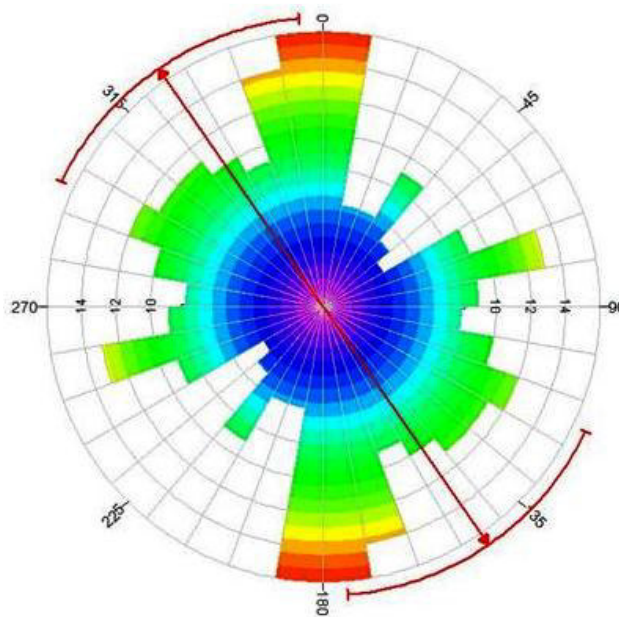


Figure 13: Rose diagram (Orientation is majorly N-S direction)

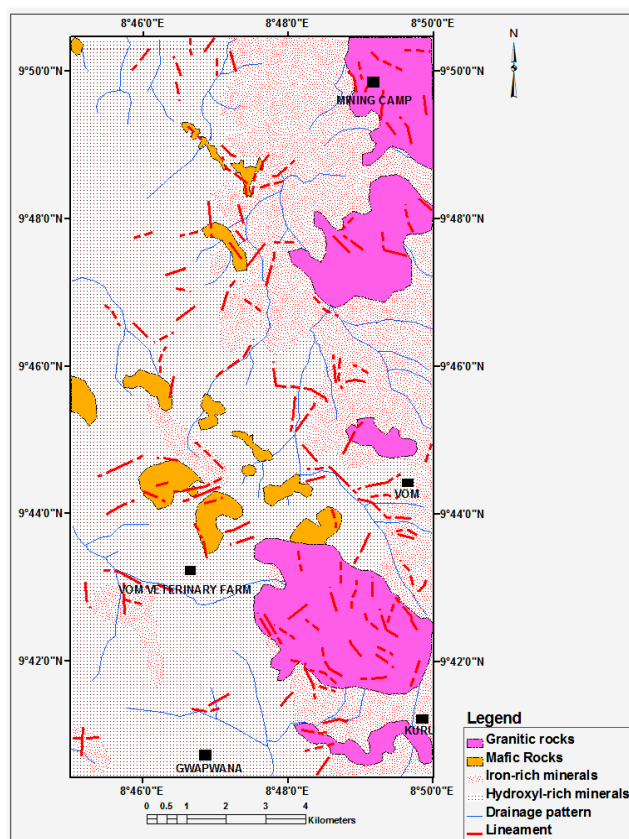


Figure 14: Geology of the study area from remotely sensed data

#### 4.2 Geological Field Mapping

Figure 15 shows seventeen (17) rock samples obtained from the study area based on exposure of rocks in the area. The rocks were physically examined at hand specimen with hand lenses and then further studied in the laboratory in order to correlate field and thin section names. It is from these comparisons that the final names of the outcrops were known. The samples were grouped into four (4) representative rock units after laboratory analyses; basalts, biotite microgranite, biotite granite and undifferentiated porphyry granite.

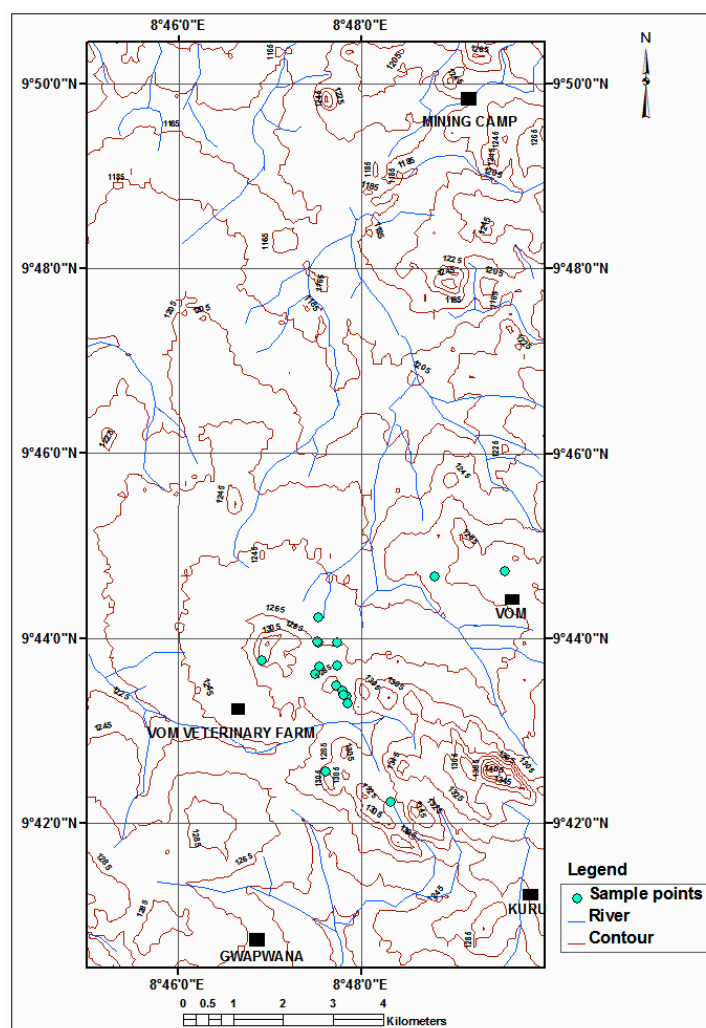
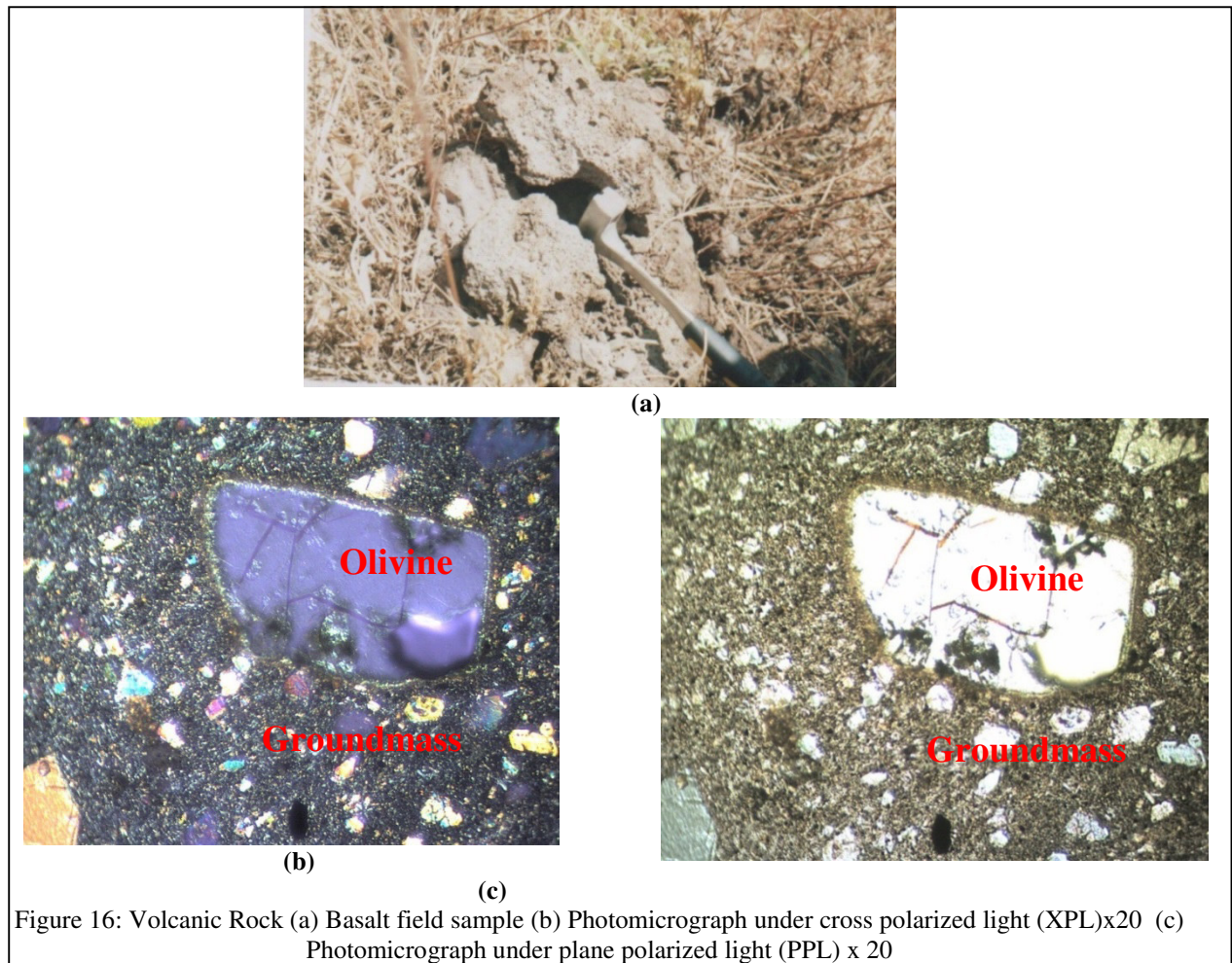


Figure 15: Sample points

#### 4.2.1 Basalts

The outcrop observed in the field is circular, hilly and not extensive with steep sloping sides. It covers about 7% of the study area. In fact, the National Veterinary Research Institute (NVRI), Vom is located within it crater. The outcrop is weathered to give rich “cotton” soil. The rock sample is massive, aphanitic and non-foliated, and therefore recognized as a volcanic rock (Figure 16a). It is basic and Melanocratic -Hypermelanic in colour due to the presence of ferromagnesian minerals. When the slide sample was microscopically observed, it contains olivine phenocryst of about 1mm in length, fresh, euhedral or slightly rounded (Figures 16a and 16c) and a ground mass composed of plagioclase (labradorite, bytownite) which is very typical of the volcanic (basalts).



#### 4.2.2 Biotite microgranite

The outcrop is located at the Northern part of the map. It is hilly and characterized by intense weathering causing a lot of cracks (fractures) that have been subsequently mineralized to form quartz veins. This outcrop covers about 25% of the study area and has a sharp contact with it adjacent biotite granite towards the west. It is holocrystalline, phaneritic and leucocratic indicating that the rock is a plutonic rock. The felsic minerals are textured as fine grained and/or equigranular (Figure 17a). The field estimated modal mineral analyses using hand lens showed that Quartz (transparent) is approximately 70%, Orthoclase (Pinkish) is 20%, Biotite (dark and shiny) is 5% and other minerals is 5%. The sample shows the characteristics of Biotite-microgranite. Microscopically, quartz appears slightly cloudy and clustered within feldspars. Albite alternate around larger crystals of labradorite. The Biotites are scattered and appeared as brown to brownish green colour to black colour (Figures 17a and 17c).

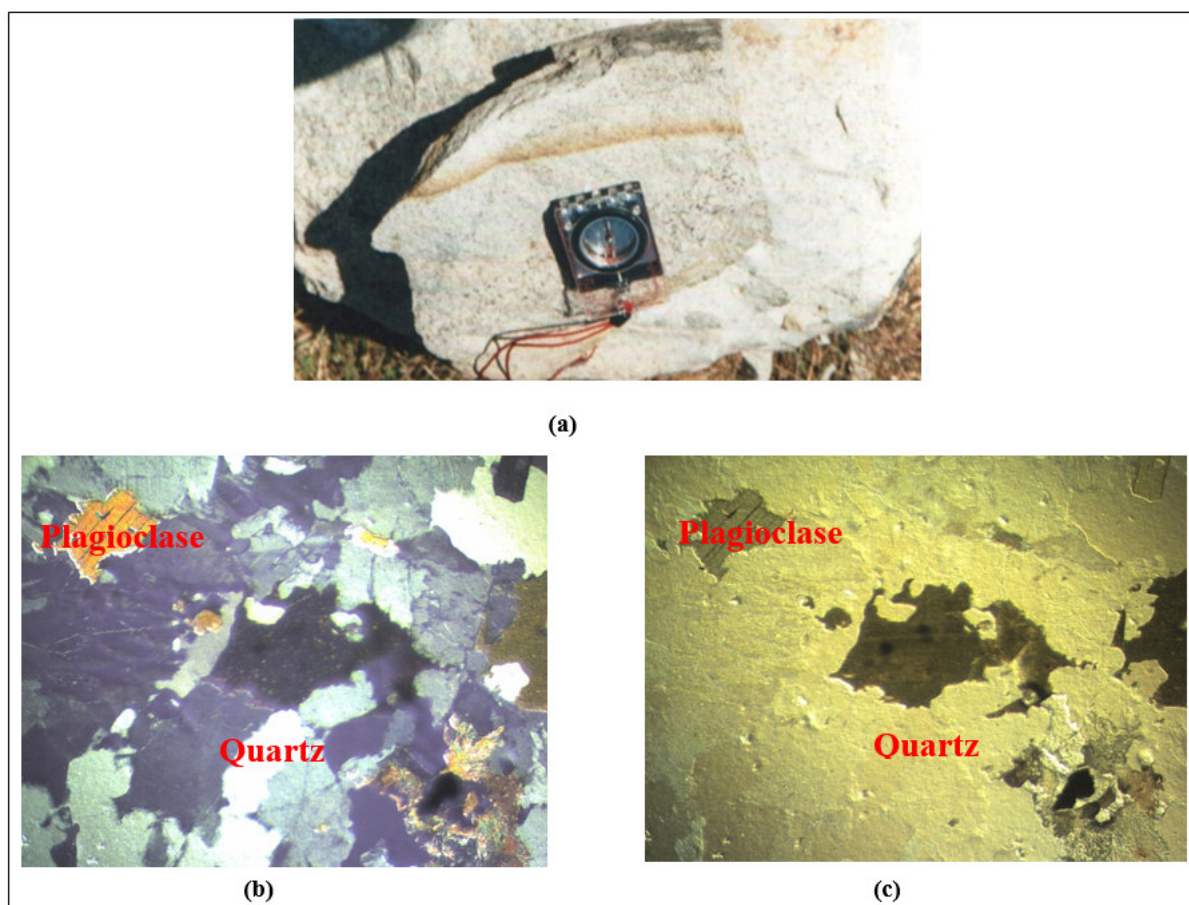


Figure 17: Plutonic Rock (a) Field sample of biotite microgranite (b) Photomicrograph under cross polarized light (XPL) x 20 (c) Photomicrograph under plane polarized light (PPL) x 20

#### 4.3.3 Biotite Granite

The outcrop extends from the Northwestern to the southeastern part of the study area. It occupies about 58% of the rock units. Even though the outcrop is quiet high, most parts of it has undergone weathering but not veined. It is holocrystalline, phaneritic and leucocratic in nature (Figure 18a). It is coarse-medium grained and highly fractured. Estimated modal mineral analyses using hand lens show that Quartz (transparent) constitute 65%, plagioclase possibly Orthoclase (Pinkish) is 30%, Biotite and others are 5%. Microscopically, it is observed that large crystals of biotite, plagioclase in the granite and quartz interlock with quartz showing sharp green boundaries between them. Quartz forms large elongated and accurate trend of subhedral crystals between large feldspars crystals. Biotite occurs as dark-brown, and dark greenish brown and disperses as fine inclusive within the feldspars (Figures 18a and 18c).

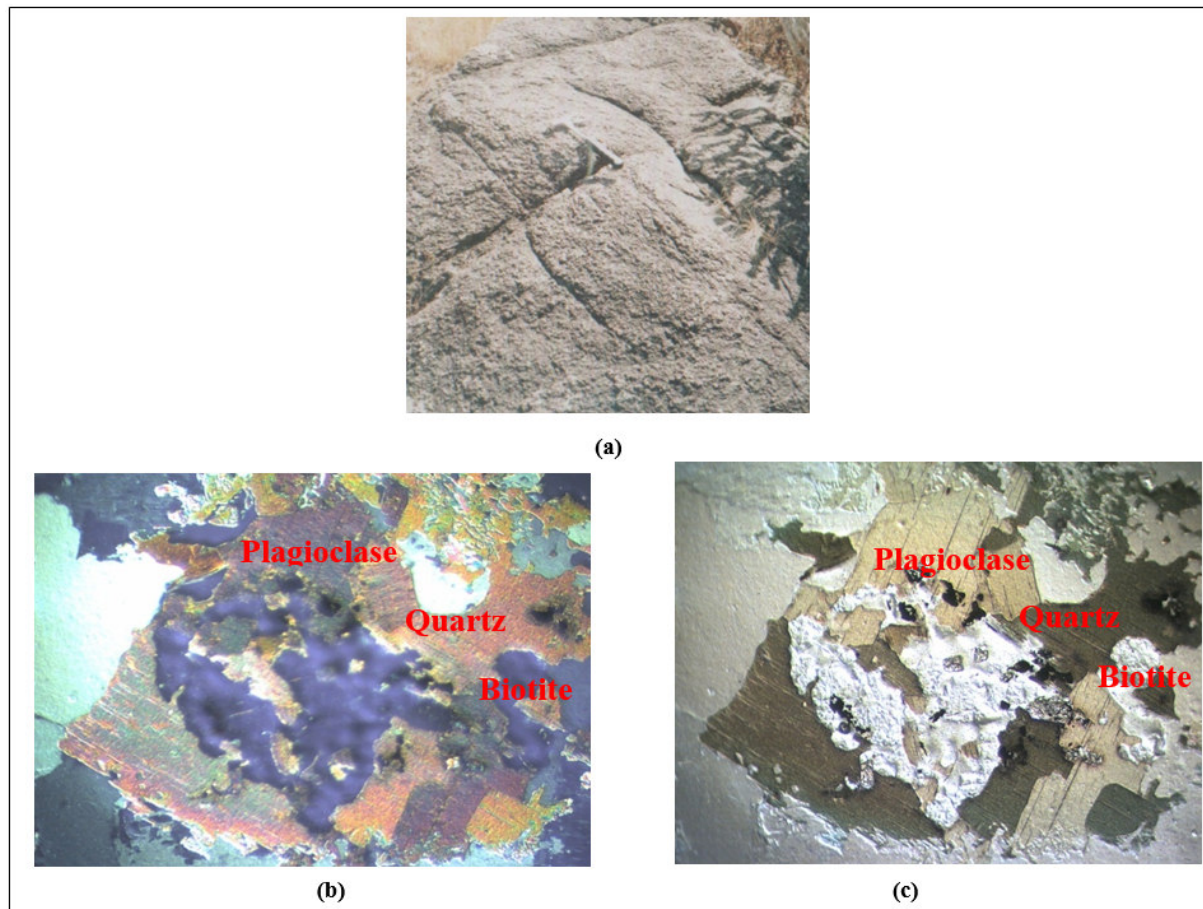
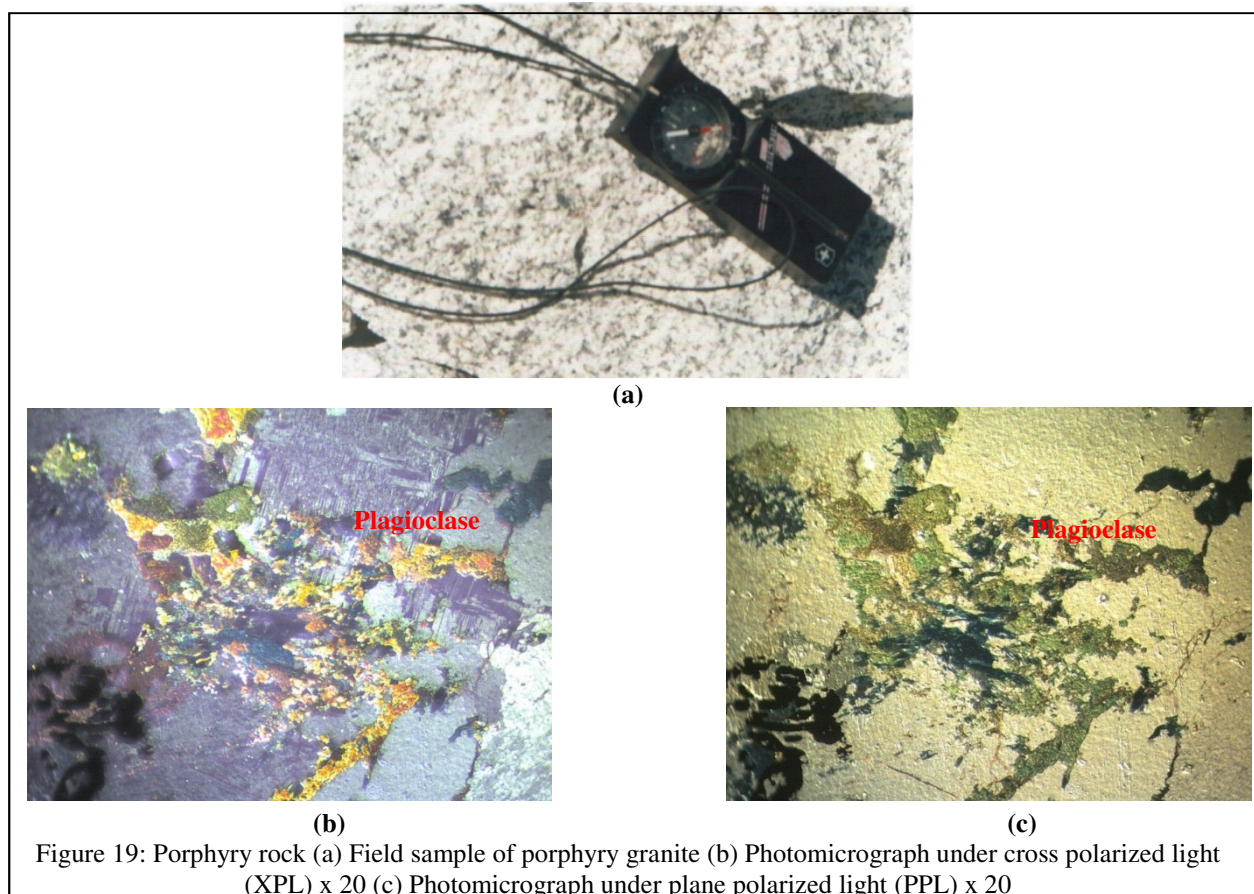


Figure 18: Plutonic Rock (a) Field sample of biotite granite (b) Photomicrograph under cross polarized light (XPL) x 20 (c) Photomicrograph under plane polarized light (PPL) x 20

#### 4.4.4 Undifferentiated Porphyry Granite

This sample is not as extensive as the others. It is characterized by small-scale lineation, which indicates intense tectonic activities as a result of younger granite intrusion. The outcrop is hilly and less affected by weathering and covers about 10% of the study area (Figure 18a). It is coarse grained with porphyries of irregular shaped minerals and scattered lineation. The estimated model mineral analysis using hand lens showed that feldspars constitutes about 25%, Quartz 45%, Hornblende approximately 20% and other accessories minerals the remaining 10%. The sample is probably an older granitic rock. Microscopically, plagioclase is observed with low relief under plane polarized and colourless in thin section with triclinic structure and simple lamellar twinning. Plagioclase may also enclose small plates of biotite, muscovite and quartz. The quartz is colourless, euhedral to subhedral with low relief under PPL (Figures 18b and 18c).

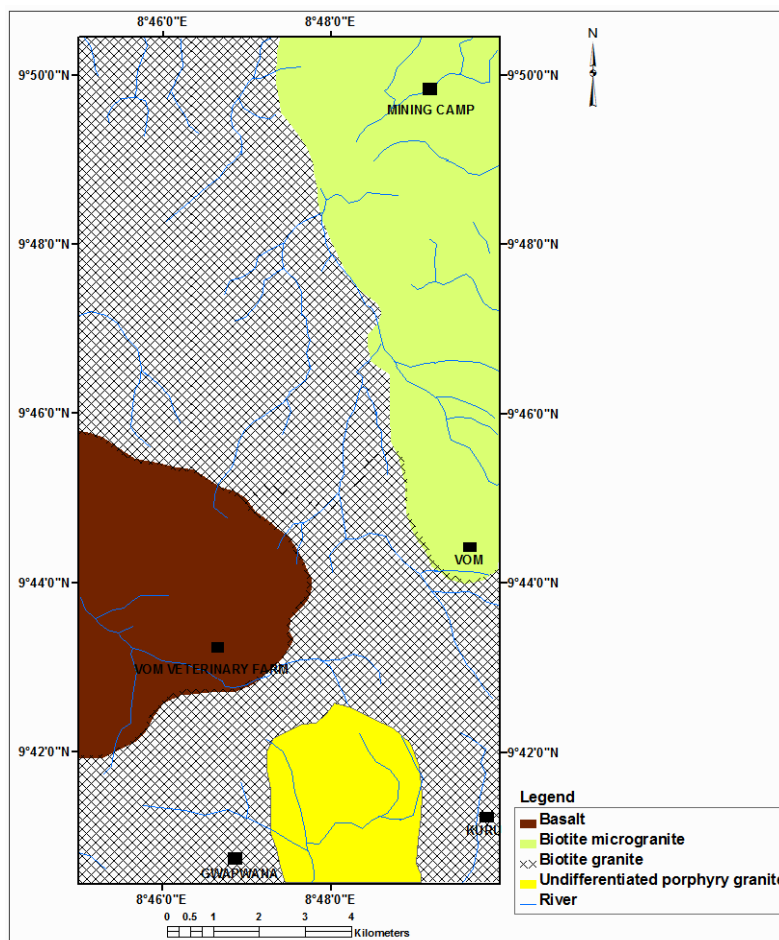
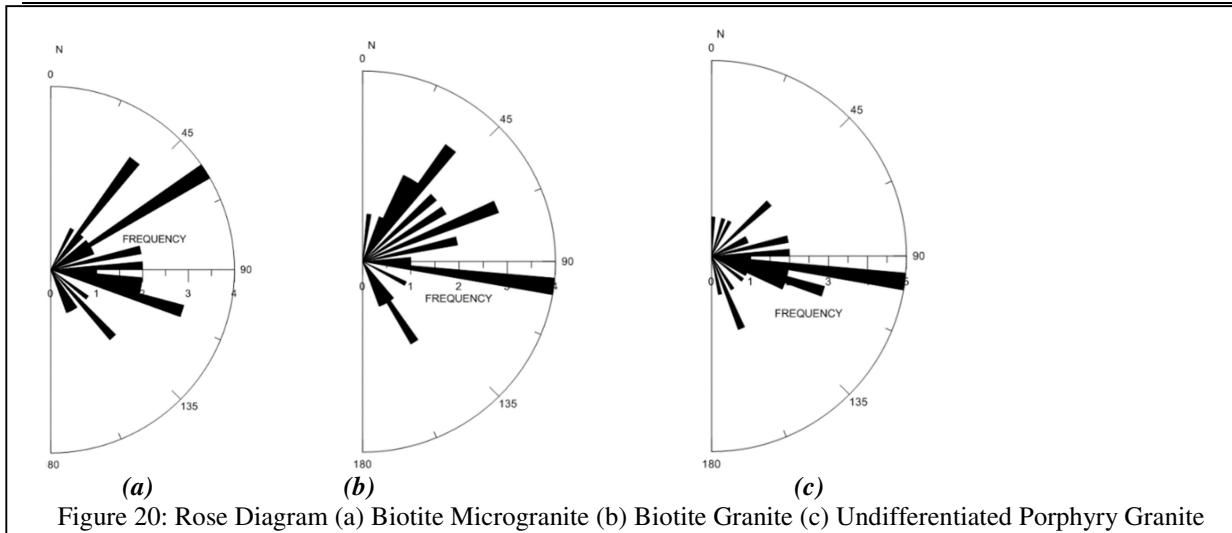


#### 4.3 Structural Analyses of the rock samples

Table 2 show the various strike orientation obtained in the field from the study area. This could have resulted from the influence of the deformational events on the basement complex underlying the younger granite most especially during the emplacement of the younger granites. All veins and vein-lets identified in the mapped area show linear trend indicative of a pre-existing well developed fissures. The outcrops in the study area generally have an average structural orientation in NE-SE direction. Figure 20a shows a structural trending majorly in the N-E direction on the biotite microgranite while biotite granite and the undifferentiated porphyry granite have structural orienting in SE directions (Figures 20b and 20c respectively). The rocks of the younger granites intruded into the Basement complex. The N-E and S-E structural trends associated with the younger granite rocks is fully shown and represented in this study area and this rocks correlates to the original structural trends of the Basement complex. Figure 21 show the digitized geological map of the study area.

Table 2: Measurement of structural features orientations

BIOTITE MICROGRANITE (°)	60, 140, 160, 150, 152, 60, 100, 80, 96, 40, 104, 26, 61, 80, 58, 110, 42, 13, 52, 110, 40, 88, 70, 108, 140, 102, 88, 92, 60, 40
BIOTITE GRANITE (°)	30, 10, 140, 160, 130, 110, 13, 60, 42, 171, 172, 112, 90, 90, 160, 80, 3, 110, 161, 80, 121, 150, 161, 50, 165, 10, 111, 60, 146, 80
UNDIFFERENTIATED PORPHYRY GRANITE (°)	108, 30, 112, 87, 48, 80, 168, 150, 50, 98, 64, 86, 160, 70, 92, 110, 160, 96, 104, 100, 102, 98, 112, 80, 126, 110, 3, 120, 100, 20



#### 4.4 Hydrogeochemical analyses and interpretations

The groundwater in this area is sourced mainly from rainfall. As the rain falls, it interacts with the various rocks and as such it dissolves most of the soluble components of the rocks. The water eventually percolates into the subsurface. Thus, the composition of groundwater is the reflection of the lithology in the area. As such, the true composition of the rocks in an area can be determined through groundwater analysis. Piper diagram can be used to determine water type (Onwuka *et al.*, 2013) and to a larger extent the petrogenesis of rocks. Five (5) groundwater samples were analyzed from the area for common major elements and the following were present  $\text{Ca}^{2+}$ ,  $\text{Mg}^{2+}$ ,  $\text{Na}^+$ ,  $\text{K}^+$ ,  $\text{HCO}_3^-$ ,  $\text{SO}_4^{2-}$  and  $\text{Cl}^-$ . Table 3 shows that the concentration of  $\text{Na}^+/\text{K}^+$  (Alkaline) ions together exceeds that of  $\text{Mg}^{2+}$  and  $\text{Ca}^{2+}$  while that of  $\text{HCO}_3^-$  (bicarbonate) exceeds that of  $\text{SO}_4^{2-}$  and  $\text{Cl}^-$ . It also shows that

the amount of alkalis and bicarbonates in the area is high and the alkali exceeds the alkaline earth metals. Figure 22 shows that the total dissolved solids (TDS) represent the total combination of all the cations and anions in parts per million (or mg/l). The analyses also indicate that the groundwater is composed mainly of alkali bicarbonate. The groundwater analyzed show that it has extensively interacted with the alkaline rocks such as the Biotite Granite, the Biotite Micro granite which are mostly alkaline in nature. Of course, these have really confirmed to the fact that field and petrography descriptions and names of the various rocks types in the study area are valid, hence given more credence to the geology map postulated by remote sensing method.

Table 3: Major Element Analyses in mg/l

S/N	Samples	pH	Temp (°c)	Mg <sup>2+</sup>	Na <sup>+</sup>	Ca <sup>2+</sup>	K <sup>+</sup>	HC0 <sup>3-</sup>	SO <sub>4</sub> <sup>2-</sup>	Cl <sup>-</sup>
1	Y1	7.06	23.40	1.33	2.84	2.09	0.74	23.40	10.04	7.00
2	Y2	7.26	22.90	0.77	13.83	1.88	4.83	20.14	12.36	5.94
3	Y3	7.50	22.60	0.33	3.41	0.78	2.58	28.00	9.71	4.99
4	Y4	7.05	22.50	0.12	3.29	0.39	2.34	22.62	11.64	6.01
5	Y5	7.02	24.00	0.19	4.10	0.69	2.69	19.26	10.98	6.20

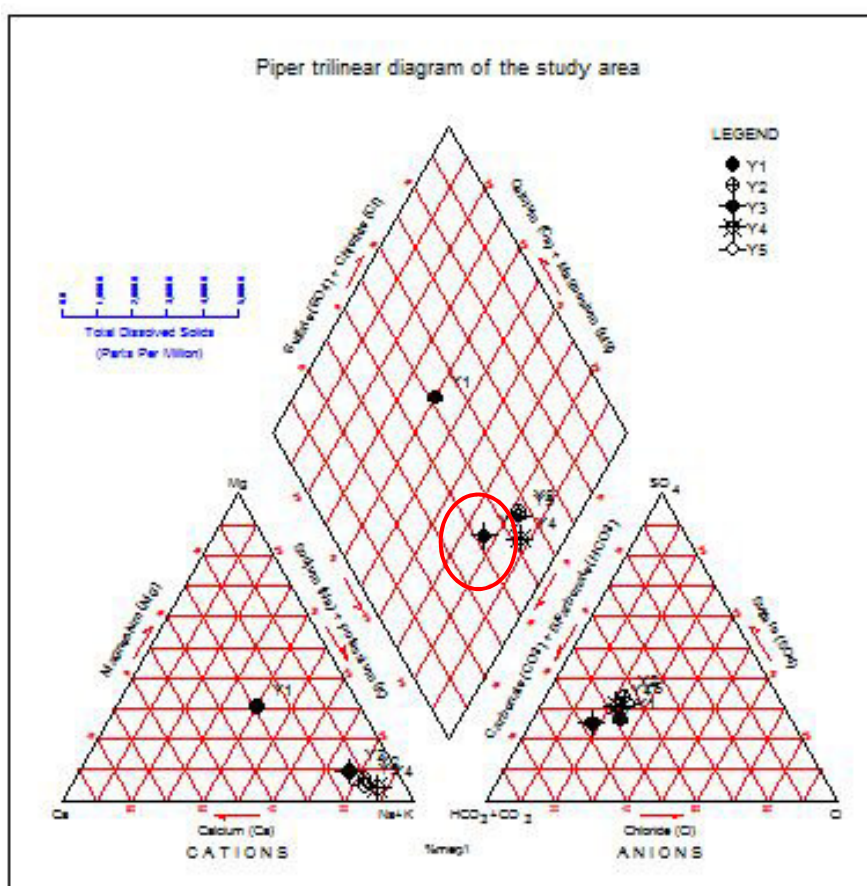


Figure 22: Piper diagram for water samples

## 5. Conclusion

The study area is a part of the Jos-Bukuru younger granite ring complex of north-central, Nigeria. Landsat data was employed in the study and five (5) land cover elements were mapped out successfully i.e. soil minerals, drainage pattern, surface water bodies, vegetations and rock outcrops. This study also delineated the mafic and granitic rocks with one hundred and twenty-four (124) lineaments on the outcrops that trend majorly in a North-south direction. The integration of the land cover map provided a viable guide for ground-truthing of the area during fieldwork. Furthermore, Seventeen (17) rock samples were obtained in the field. They were studied, analyzed and four (4) basic rocks units were identified as basalt, biotite microgranite, biotite granite and undifferentiated older (porphyry) granite. The fractures found on the biotite microgranite trend majorly in the N-

E direction while those of biotite granite and the undifferentiated porphyry granite strike mainly in S-E direction. It is important to note that the basaltic outcrops do not have distinct fractures. Furthermore, five (5) groundwater samples were analyzed for major elements using Atomic Absorption Spectrometer (AAS) and the result indicated the presence  $\text{Ca}^{2+}$ ,  $\text{Mg}^{2+}$ ,  $\text{Na}^+$ ,  $\text{K}^+$ ,  $\text{HCO}_3^-$ ,  $\text{SO}_4^{2-}$  and  $\text{Cl}^-$  of which the alkali-bicarbonate dominated the major composition of the groundwater as plotted on piper trilinear diagram. Hence, the major elements show that the total concentration of  $\text{Na}^+ > \text{K}^+ > \text{Ca}^{2+} > \text{Mg}^{2+}$  while  $\text{HCO}_3^- > \text{SO}_4^{2-} > \text{Cl}^-$ . This result proved valid for the geology of the study area as it is composed predominantly of rocks that are mainly alkaline in nature. Conclusively, there is an interrelationship between geological mapping by remote sensing and field work. The study has further shown beyond doubt that remote sensing is a viable tool in geological mapping most especially when verified by fieldwork.

### Acknowledgements

The authors want to appreciate Prof. T.C Davies for his guidance, suggestions and constructive criticism of the work. We are also grateful to the Department of Geology and Mining, University of Jos, and the National Metallurgical Development Center (NMDC), Jos, for thin section and water sample analyses respectively as well as Global Land Cover Facilities for allowing us have access to their data. Thus, we sincerely appreciate the people of Vom and Kuru towns for their hospitality, support and assistance during the field work despite daunting challenges in the communities.

### References

- Adam, J.B. & Felic, A.L., (1967). Spectral reflectance 0.4–2.0 micron of silicate rock powders. *Journal of Geophysical Research* 72, 5705–5715.
- Bowden P. & Turner D.C (1974). Origin of the Younger Granites of Northern Nigeria. *Countr. Miner, petrol* Vol25, pp153-162.
- Carranza, E.J.M. & Hale, M. (2002). Mineral imaging with Landsat Thematic Mapper data for hydrothermal alteration.
- Clar I. (2015). Groundwater Geochemistry and Isotopes. Government works VD:20150302. International Standard Book Number-13:978-1-4665-9174-5 (eBook - PDF). PP. 16.
- Darning, W.P (1998). Affiliated Research Center, Integrated Use of Remote Sensing and GIS for Mineral Exploration. Final Report, pp. 3 – 4.
- David W. L & Woil M. M. (2012). Landsat-TM-Based Discrimination of Lithological Units Associated with the Purtunig Ophiolite, Quebec, Canada. *Remote Sens.* 2012, 4, 1208-1231; doi:10.3390/rs4051208. ISSN 2072-4292.
- Drury S.A (1993) *Image Interpretation in Geology*, 2:145 – 149, 225 – 231.
- Drury, S.A. & Berhe, S.M. (1993) Accretion tectonics in northern Eritrea revealed by remotely sensed imagery. *Geological Magazine*, v.130, p.177-190.
- Falconer J.D. (1921). The geology and geography of Northern Nigeria, Macmillan, London.
- Falconer J.D & Reaburn.C. (1923). The Northern Tin Fields of Bauchi Province: Bulletin C.S.N NO 4.
- Jacobson R.R.E, Macleod W.N. & Black R (1958). Ring Complexes in the Younger Granite Province of Northern Nigeria. *Memo geol Soc. Land. Vol 1* Pp 72.
- Lillesand, T.M. & Kiefer, R.W. (1994). *Remote Sensing and Image Interpretation*, 3rd Edition. John Wiley & Sons, New York, 750 p.
- Macleod W.N & Berridge N.G (1971). The Younger Granites in Geology of the Jos-Plateau, Vol 2, *Bulletin. Geology survey of Nigeria* 32, Pp 67-84.
- Macleod W.N., Turner D.C & Wright E.P. (1971). The geology of the Jos Plateau Vol 1 general Geology Bulletin NO. 32.
- Mackay R.A. Greenwood .R & Rockingham J.E (1949). The Geology of the Plateau Tin Fields, Resurvey. *Geol. Survey Nig Bull. No 32* vol 1 Pp116.
- Malomo S. (2009). Fieldwork, the core of geological practice. Keynote address: In proceedings of field mapping standization workshop. Pp 15-17
- Mshiu E.E (2011). Landsat Remote Sensing Data as an Alternative Approach for Geological Mapping in Tanzania: a case study in the Rungwe volcanic province, south-western Tanzania. *Tanz. J. Sci.* Vol. 37 2011, pp 26-36.
- Onwuka O.S., Ekwe A.C. & Adimonye, O.J. (2013). Geoelectrical and Hydrogeochemical Assessment of the Groundwater Potentials of Ehandiagu, Enugu State, Southeastern Nigeria. *Jordan Journal of Earth and Environmental Sciences*. Volume 5, Number 2, December. 2013 ISSN 1995-6681 Pages 63- 71.
- Qari M.H.T., Madani A.A., Matsah M.I.M., & Hamimi Z., (2007). Utilization of ASTER and Landsat Data in Geologic Mapping of Basement Rocks of Arafat Area, Saudi Arabia. *The Arabian Journal for Science and Engineering*, Volume 33, Number 1C.

- Rothery, D.A. (1987). Improved discrimination of rock units using Landsat Thematic Mapper imagery of the Oman ophiolite. *J. Geol. Soc. London* 1987, 144, 587-597.
- Rowan, L.C., Mars, J.C., & Simpson, C.J. (2005). Lithologic mapping of the Mordor, NT, Australia ultramafic complex by using the Advanced Spaceborne Thermal Emission and Reflection Radiometer (ASTER). *Remote Sens. Environ.* 2005, 99, 105-126.
- Sabreen G., & Timothy K. (2006). Lithological mapping in the Eastern Desert of Egypt, the Barramiya area, using Landsat thematic mapper (TM). [www.elsevier.com/locate/jafrearsci](http://www.elsevier.com/locate/jafrearsci). *Journal of African Earth Sciences* 44 (2006) 196–202.
- Sabins F.F., (1996). *Remote Sensing Principles and Interpretation*, Third Ed. Freeman & Co, New York, USA, 449p.
- Souza Filho, C.R. & Drury. SA (1997). Remote sensing strategies for lithological mapping of Pan African assemblages in arid environments - a case study in Eritrea, NE Africa. *Bol./G-USP, Ser.Gent.*28:1-22
- Sultan, M., Arvidson, R.E., Sturchio, N.C. & Guinness, E.A. (1987). Lithological mapping in arid regions with Landsat thematic mapper data: Meatiq dome, Egypt. *Geological Society American Bulletin*, v. 99, p.748-762.

The IISTE is a pioneer in the Open-Access hosting service and academic event management. The aim of the firm is Accelerating Global Knowledge Sharing.

More information about the firm can be found on the homepage:

<http://www.iiste.org>

### CALL FOR JOURNAL PAPERS

There are more than 30 peer-reviewed academic journals hosted under the hosting platform.

**Prospective authors of journals can find the submission instruction on the following page:** <http://www.iiste.org/journals/> All the journals articles are available online to the readers all over the world without financial, legal, or technical barriers other than those inseparable from gaining access to the internet itself. Paper version of the journals is also available upon request of readers and authors.

### MORE RESOURCES

Book publication information: <http://www.iiste.org/book/>

Academic conference: <http://www.iiste.org/conference/upcoming-conferences-call-for-paper/>

### IISTE Knowledge Sharing Partners

EBSCO, Index Copernicus, Ulrich's Periodicals Directory, JournalTOCS, PKP Open Archives Harvester, Bielefeld Academic Search Engine, Elektronische Zeitschriftenbibliothek EZB, Open J-Gate, OCLC WorldCat, Universe Digital Library , NewJour, Google Scholar

